A THREE-DIMENSIONAL BOUNDARY ELEMENT MODEL FOR EDDY CURRENT NDE

R. E. Beissner

Southwest Research Institute
6220 Culebra Road
San Antonio, Texas 78284

INTRODUCTION

The long-range objective of the work reported here is to provide a theoretical basis for the prediction of the probability of flaw detection in eddy current nondestructive evaluation (NDE). As demonstrated in a previous communication [1], much of the labor involved in probability of detection analyses can be transferred to a computer if one has available a reliable algorithm for the prediction of flaw signals as a function of flaw size and shape, probe geometry, and the other parameters defining an eddy current inspection. Because there is no simplifying symmetry in the interaction of a general eddy current field with a flaw of arbitrary shape and position, the model used for flaw signal predictions must be three dimensional, and capable of predicting the probe impedance change for a flaw at an arbitrary position in the field of an eddy current probe. The immediate objective of the present work is to develop such a three-dimensional model.

In previous publications [1-3], a computational approach based on the boundary element method (BEM) [4] was used to numerically solve Maxwell's equations for the electric and magnetic fields on the surface of a flaw in an electrically conducting medium. The fields thus calculated were then used to compute the probe impedance change associated with the flaw according to the reciprocity integral given by Auld [5]. While this approach is, in principle, capable of providing probe impedance predictions in all situations of concern in eddy current NDE, its use requires a large computer memory and long computation times for all but the simplest geometries. It was this shortcoming of the original approach that motivated the search for a more efficient method based on an approximate formulation of the eddy current problem.

The approach described here, and in preliminary form in previous publications [6-8], makes use of the magnetic scalar potential to describe the field outside the conductor and inside the volume of a surface-breaking flaw. Direct solution of Maxwell's equations inside the conductor is avoided by use of an approximate boundary condition on the normal derivative of the potential at the conductor surface. Formulation of the problem in this way, through the calculation of the scalar potential with an approximate boundary condition, is similar to the approach used by others [9] in successful predictions of the impedance changes caused by

flaws of simple geometry. The present method differs from those used earlier in the introduction of a more general boundary condition and in application of the BEM, which allows treatment of complex flaw and part geometries. The end result is a numerical method computationally simpler than the exact BEM solution of Maxwell's equations, and applicable to a more general class of problems than earlier formulations based on magnetic scalar potential theory.

The theoretical basis of the scalar potential approach with an approximate boundary condition is outlined in the next section. This is followed by a description of the BEM, which reduces the boundary integral equation for the potential to a system of algebraic equations solvable on a computer. Next, numerical examples of impedance loci are presented for eddy current probe scans over simple three-dimensional conductors with and without flaws. The paper concludes with a summary of the present state of development of the method and a discussion of problems requiring further work.

SCALAR POTENTIALS AND THE IMPEDANCE BOUNDARY CONDITION

In the quasistatic approximation, Maxwell's equation for the magnetic field $\vec{H}$ is

$$\nabla \times \vec{H} = \vec{j}, \tag{1}$$

where $\vec{j}$ is the current density. With reference to Fig. 1, the current density vanishes in the region V, which is bounded by the surface S of the conductor, a surface around the eddy current probe, and a closure surface S_1. It follows that

$$\vec{H}(\vec{x}) = -\nabla\phi(\vec{x}) \tag{2}$$

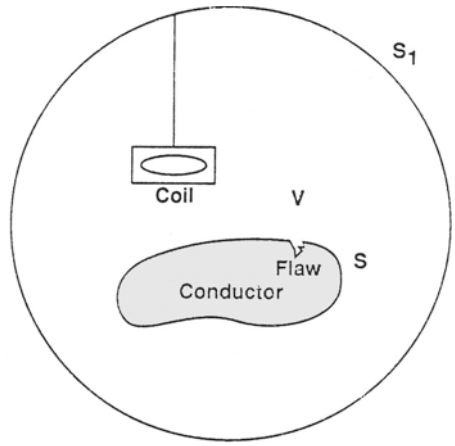

Fig. 1. Geometry for the magnetic scalar potential formulation of the eddy current problem. The scalar potential is defined only in the volume V where the current density vanishes.

for $\vec{x}$ in V because the curl of $\vec{H}$ vanishes in V. From the condition that the divergence of $\vec{H}$ vanishes in free space, one finds that the magnetic scalar potential $\Phi(\vec{x})$ satisfies Laplace's equation for x in V.

One of the boundary conditions needed to calculate $\Phi(\vec{x})$ is provided by the radiation condition on $\vec{H}(\vec{x})$, which must be satisfied for $\vec{x}$ on S_1 as S_1 recedes to infinity. In most applications of scalar potential theory, the second condition is provided by matching the exterior solution $\Phi(\vec{x})$ to an interior solution for the potential inside S according to some physical condition imposed on the potential or its normal derivative. However, except in certain special cases, such as the case of a perfect conductor where the normal derivative of Φ must vanish on S, the usual procedure is not applicable to the eddy current problem. This is because the current density $\vec{j}$ does not vanish inside S, and the interior solution cannot be expressed in terms of a scalar potential. Calculation of the exact exterior potential requires solution of the vector field equations inside the conductor with tangential components of the magnetic field matched at the surface.

To avoid this difficulty, it is necessary to impose an approximate boundary condition on the potential or its normal derivative on the conductor surface S. The simplest such condition is that the normal derivative vanish, as noted above. This leads to the solution for a perfect conductor with vanishing skin depth, which, as shown by Burke [10], can be used to calculate the probe impedance to first order in the actual skin depth of the material. Applications of this perturbation approach to eddy current flaw problems are discussed elsewhere [8,10].

In the present work, a more general boundary condition is used that is applicable to magnetic as well as nonmagnetic materials, and is valid for arbitrary values of the conductivity. It is, however, based on the assumptions that the surface at any point can be approximated by its tangent plane at that point, and that the field varies much more slowly in tangential directions than in the normal direction. Under these conditions, it can be shown that the tangential components of the electric and magnetic fields, which are taken to have time dependence $e^{i\omega t}$, are related by the well-known impedance boundary condition [11]

$$\vec{E} \sim \frac{1+i}{2}\omega\mu_r\delta\vec{n} \times \vec{H}, \tag{3}$$

where ω is the angular frequency, μ_r is the relative permeability, δ is the skin depth, and $\vec{n}$ is the unit normal to the surface. As Senior [12] and Nicholas [13] have shown, the equivalent condition on the normal derivative of the magnetic scalar potential is

$$\frac{d\Phi}{dn} \sim -\frac{1}{2}(1-i)\mu_r\delta\left(\frac{d^2\Phi}{dt_1^2} + \frac{d^2\Phi}{dt_2^2}\right), \tag{4}$$

where d/dt_1 and d/dt_2 denote tangential derivatives. As will be shown in the next section, this relationship can be incorporated in a straightforward way in the BEM formalism as a boundary condition relating $d\Phi/dn$ to Φ at neighboring mesh points, thus providing the condition needed to compute Φ on the conductor surface. For further discussion of the implications of this boundary condition in certain limiting cases, see Ref. 9.

Once Φ has been determined on the conductor surface, and its normal derivative calculated from Eq. (4), the impedance of an eddy current probe can be evaluated. The expression needed for the impedance calculation follows from the reciprocity integral [5], which is usually written as

$$\Delta Z = \frac{1}{I^2}\int_S (\vec{E}_0 \times \vec{H} - \vec{E} \times \vec{H}_0)\cdot \vec{n}\, dS \tag{5}$$

where I is the excitation current, ΔZ is the change in impedance relative to the probe impedance in free space, and zero subscripts denote fields in free space. From Eq. (1) a vector identity and Maxwell's equation for the curl of $\vec{E}$, one obtains

$$\begin{aligned}\vec{n}\cdot\vec{E}_0 \times \vec{H} &= \vec{n}\cdot\nabla\Phi \times \vec{E}_0 \\ &= -\Phi\vec{n}\cdot\nabla\times\vec{E}_0 + \vec{n}\cdot\nabla\times(\vec{E}_0\Phi) \\ &= i\omega\mu_0\Phi\vec{n}\cdot\vec{H}_0 + \vec{n}\cdot\nabla\times(\vec{E}_0\Phi).\end{aligned} \tag{6}$$

When the integral of the last term in Eq. (6) is changed to a volume integral by means of the divergence theorem, the integrand becomes the divergence of the curl of a vector, which vanishes. Thus, substitution of Eq. (6) in Eq. (5) gives

$$\Delta Z = -\frac{i\omega\mu_0}{I^2}\int_S \left[\Phi\frac{d\Phi_0}{dn} - \Phi_0\frac{d\Phi}{dn}\right]dS \tag{7}$$

where Φ_o is the potential in free space.

BOUNDARY ELEMENT SOLUTION FOR THE SCALAR POTENTIAL

Application of Green's theorem to Laplace's equation for $\Phi(\vec{x})$ yields an integral expression for $\Phi(\vec{x})$ in terms of the potential and its normal derivative on S. In the limit as $\vec{x}$ approaches a point on S, this becomes the following integral equation for Φ on S [7,14]:

$$\Gamma(\vec{x})\Phi(\vec{x}) = \Phi_0(\vec{x}) + \int_S \left[G_0(\vec{V},\vec{x}')\frac{d\Phi(\vec{x}')}{dn} - \Phi(\vec{x}')\frac{dG_0(\vec{x},\vec{x}')}{dn}\right]dS \tag{8}$$

where G_o is the free-space Green's function, the integral on the right side is a Cauchy principal value, and $\Gamma(\vec{x})$ is a function of the solid angle subtended by S at $\vec{x}$ [14]. A more convenient equivalent equation for numerical solution is [7]

$$\Phi(\vec{x}) = \Phi_0(\vec{x}) + \int_S \left[G_0(\vec{x},\vec{x}')\frac{d\Phi(\vec{x}')}{dn} - (\Phi(\vec{x}') - \Phi(\vec{x}))\frac{dG_0(\vec{x},\vec{x}')}{dn}\right]dS, \tag{9}$$

in which the quantity $\Phi(\vec{x}')$-$\Phi(\vec{x})$ on the right side reduces the order of the singularity in dG_o/dn, thus avoiding numerical difficulties associated with the principal value integral in Eq. (8) [4].

To solve Eq. (9) by the BEM, the integral over the surface S is written as the sum of integrals over a mesh of boundary elements as indicated in Fig. 2. Within each element, the surface is defined in terms of two parameters ξ_1 and ξ_2, each having values between -1 and 1. Thus,

$$\vec{x}(\xi_1,\xi_2) = \sum_Q M_Q(\xi_1,\xi_2)\vec{x}_Q \tag{10}$$

where the M_Q are given shape functions [4] and the $\vec{X}_Q$ are the known values of $\vec{X}$ at each node Q on the periphery of the element, as indicated in Fig. 2. The unknown function $\Phi(\vec{x})$ is assumed to vary within each element in a similar way,

$$\Phi(\vec{x}(\xi_1,\xi_2)) = \sum_Q M_Q(\xi_1,\xi_2)\Phi_Q, \tag{11}$$

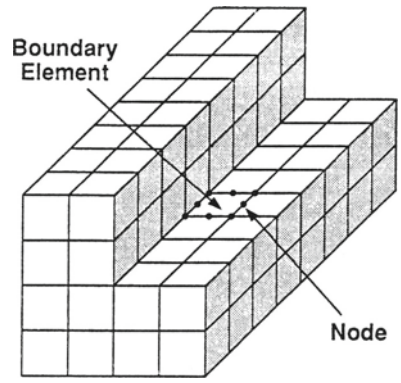

Fig. 2. Discretization by the boundary element method. The surface of the conductor is represented as a mesh of surface elements with nodal points on the boundaries of each element.

and its tangential derivatives, according to Eqs. (10) and (11), are

$$\frac{d^2\Phi}{dt_i^2} = \frac{\sum_Q \frac{d^2 M_Q(\xi_1,\xi_2)}{d\xi_i^2}\Phi_Q}{|\sum_Q \frac{dM_Q(\xi_1,\xi_2)}{d\xi_i}\vec{x}_Q|^2}, \tag{12}$$

with i = 1, 2 [7]. Substitution of Eq. (12) in Eq. (4) leads to the following expression for the normal derivative:

$$\frac{d\Phi}{dn} = \sum_Q N_Q(\xi_1,\xi_2)\Phi_Q, \tag{13}$$

with

$$N_Q(\xi_1,\xi_2) = -\frac{1}{2}(1-i)\mu_r\delta\sum_{i=1}^{2}\frac{\frac{d^2 M_Q}{d\xi_i^2}}{|\sum_Q \frac{dM_Q}{d\xi_i}\vec{x}_Q|^2}. \tag{14}$$

Finally, with $\vec{x}$ at node P, substitution of Eqs. (11) and (14) in Eq. (9) gives

$$\begin{aligned}\Phi_P =& \Phi_P^0 + \sum_\alpha\sum_Q \Phi_Q \int_{-1}^{1}\int_{-1}^{1}\Big[G_0(\vec{x}_P,\vec{x}'(\xi_1,\xi_2))N_Q(\xi_1,\xi_2) \\ &- (M_Q(\xi_1,\xi_2)-\delta_{PQ})\frac{dG_0(\vec{x}_P,\vec{x}'(\xi_1,\xi_2))}{dn}\Big]J_\alpha(\xi_1,\xi_2)d\xi_1 d\xi_2\end{aligned} \tag{15}$$

where the sum on α is the sum over boundary elements; $J_\alpha(\xi_1,\xi_2)$ is the Jacobian of the transformation from $\vec{x}$ to ξ_1,ξ_2; and δ_{PQ} is the Kronecker delta. Evaluation of the integral in Eq. (15) is accomplished by double Gaussian quadrature when nodes P and Q are in different elements, and by the method described by Rizzo and Shippy [4] when P and Q are in the same element. The end result is a discretized set of linear algebraic equations for the potentials Φ_P at each node in the system. If Φ and Φ_O represent the column vectors of Φ_P and Φ_P^0 at each node, then the matrix form of the system of equations is

$$A\Phi = \Phi_0 \tag{16}$$

where A is an NxN complex matrix for a system with N nodes.

Once the potential has been computed, evaluation of the impedance integral is straightforward. From Eqs. (7), (11), and (13), the impedance change is

$$\Delta Z = -\frac{i\omega\mu_0}{I^2}\sum_{\alpha}\sum_{Q}\Phi_Q\int_{-1}^{1}\int_{-1}^{1}\left[M_Q(\xi_1,\xi_2)\frac{d\Phi_0}{dn} - \Phi_0 N_Q(\xi_1,\xi_2)\right]J_\alpha(\xi_1,\xi_2)\,d\xi_1\,d\xi_2 \tag{17}$$

where Φ_o and its normal derivative at ξ_1,ξ_2 are expressed in terms of nodal values and shape functions according to Eq. (11).

As can be seen from Eq. (15), the BEM matrix A is independent of the incident field Φ_o. It follows that once the inverse of A (or, equivalently its LU decomposition) has been computed, the potential Φ is easily determined for any incident field by application of the inverse to the vector Φ_o (or back substitution if the LU decomposition is saved). This feature is particularly convenient in probability of detection applications where one needs a large number of calculations of ΔZ as a function of probe position with respect to the flaw position. Such applications require only one BEM solution applied to different Φ_o vectors for each probe location.

COMPUTATIONS OF IMPEDANCE LOCI

As examples of applications of the method, ΔZ loci for eddy current scans over three-dimensional objects have been computed with and without flaws. The first example is the cube shown in Fig. 3, in which a single turn coil is scanned over the top of the piece, once with no flaw present, and again with a cubic indentation in the top face. The conductor in this case is a cube of aluminum with a 2-cm edge dimension, and the frequency is 100 kHz; other dimensions are shown approximately to scale in Fig. 3. Impedance loci are shown in Fig. 4 for scans that originate 1 cm off the back edge of the cube and terminate with the probe centered over the top face. The labels *NF* and *F* refer to scans with no flaw and with a flaw in the center of the top face, respectively, as shown in Fig. 3. The flaw signal, which is the difference between the *F* and *NF* curves, is quite large in this case, as one would expect because the flaw is large.

The geometry for the second example is shown in Fig. 5. Here the piece is 4 cm long and 2 cm deep, with a 4 x 2 x 2-cm block removed to form a step in the piece. The flaw is a rectangular corner notch cut into the two faces of the step. There are two scans in this case, one over the top edge and the other near the center of the horizontal face of the step, both beginning on the back edge of the piece and ending halfway along its length. Again, the coil, flaw, and liftoff dimensions are approximately to scale; and the material and frequency are the same as in the first example.

From the geometry shown in Fig. 5, one would expect to see smaller changes associated with the flaw in the scan over the top edge than in the scan over the step because the probe is much closer to the flaw in the latter case. The expected result was obtained from the numerical model, as evidenced by the impedance loci shown in Fig. 6.

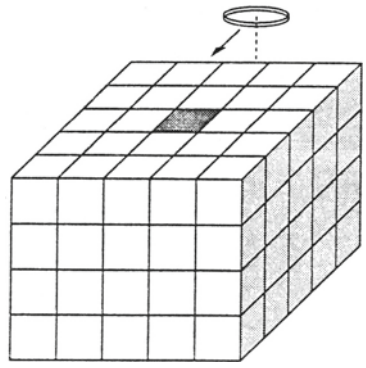

Fig. 3. Geometry for the first example of a probe impedance calculation. A circular coil is scanned over the top of a conducting cube; the dark area represents a cubic indentation (flaw) in the top face.

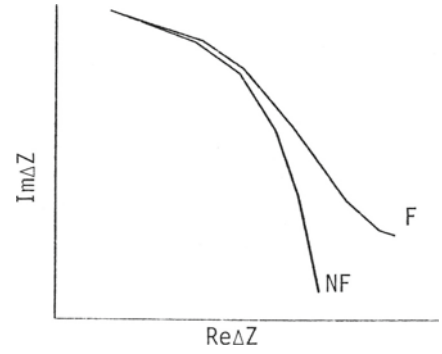

Fig. 4. Impedance loci for the scan shown in Fig. 3. The impedance change ΔZ is the change relative to the probe impedance in free space; *F* and *NF* refer to scans with and without the flaw indicated in Fig. 3.

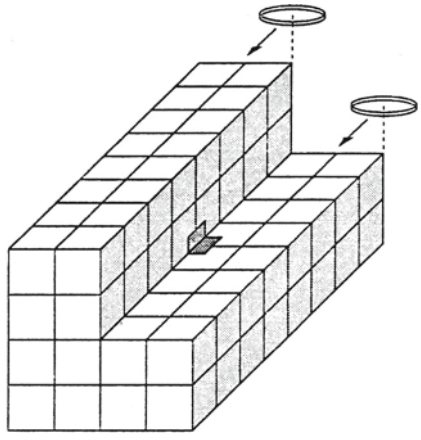

Fig. 5. Geometry for the second example of a probe impedance calculation. The dark area represents a corner flaw cut into the vertical and horizontal faces of the piece. Two scans are considered, one over the top edge and another over the horizontal face of the step.

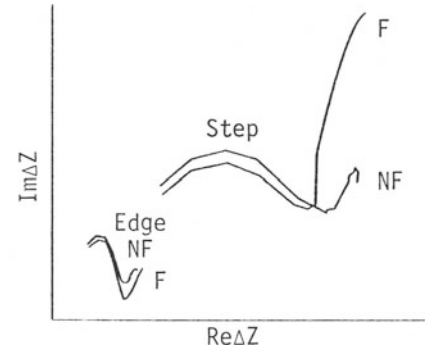

Fig. 6. Impedance loci for the scans shown in Fig. 5. The labels EDGE and STEP refer to the upper and lower scans, respectively, indicated in Fig. 5. The STEP scan produces a larger flaw signal because the probe is closer to the flaw.

CONCLUSIONS AND PLANS FOR FURTHER DEVELOPMENT

The numerical examples presented here were intended as qualitative tests of the model to determine if it is numerically practical, and if it produces physically reasonable predictions of impedance loci. While the results shown in Figs. 4 and 6 are certainly not exhaustive, they do provide some evidence that predictions are in accord with expectations and are, therefore, physically reasonable.

Along with the effort to improve the efficiency of the code, future work will be devoted to determination of the accuracy of its predictions

of probe impedance. This will involve comparisons with experimental data, and with predictions based on analytic solutions for simple geometries and other numerical methods for more complex cases.

ACKNOWLEDGMENTS

All of the numerical work reported here was performed on the CRAY-2 at Harwell Laboratory, UKAEA, during my temporary attachment to the Laboratory. I wish to thank the Harwell staff for their hospitality, and acknowledge several helpful discussions with J. A. G. Temple and C. C. Holt. This work was supported in part by the Center for Advanced Nondestructive Evaluation, operated by the Ames Laboratory, USDOE, for the Air Force Wright Aeronautical Laboratories/Materials Laboratory under Contract No. W-7405-ENG-82 with Iowa State University.

REFERENCES

1. R. E. Beissner, K. A. Bartels, and J. L. Fisher, "Prediction of the Probability of Eddy Current Flaw Detection," in Review of Progress in Quantitative NDE, edited by D. O. Thompson and D. E. Chimenti (Plenum, New York, 1988), Vol. 7.
2. R. E. Beissner, "Eddy Current Response to Three-Dimensional Flaws by the Boundary Element Method," in Review of Progress in Quantitative NDE, edited by D. O. Thompson and D. E. Chimenti (Plenum, New York, 1987), Vol. 6A.
3. R. E. Beissner, "Boundary Element Model of Eddy Current Flaw Detection in Three Dimensions," J. Appl. Phys. 60, 352 (1986).
4. F. J. Rizzo and D. J. Shippy, "An Advanced Boundary Integral Equation Method for Three-Dimensional Thermoelasticity," Int. J. Num. Methods Eng. 11, 1753 (1977).
5. B. A. Auld, "Theoretical Characterization and Comparison of Resonant Probe Microwave Eddy Current Testing with Conventional Low Frequency Eddy Current Methods," in Eddy Current Characterization of Materials and Structures, ASTM STP 722, edited by G. Birnbaum and G. Free (American Society for Testing and Materials, Philadelphia, 1981), p. 332.
6. R. E. Beissner, "A Boundary Element Model for Eddy Current NDE," in Proceedings of the Third National Seminar on Ferromagnetic NDE, edited by S. Marinov (Western Atlas Co., Houston, 1988).
7. R. E. Beissner, "Scalar Potential Model of Eddy Current Interactions with Three-Dimensional Flaws," submitted to Journal of Nondestructive Evaluation.
8. R. E. Beissner, "Approximate Model of Eddy Current Probe Impedance for Surface-Breaking Flaws," submitted to Journal of Nondestructive Evaluation.
9. A. M. Lewis, D. H. Michael, M. L. Lugg, and R. Collins, "Thin-Skin Surface Fields in Electromagnetic Methods of Crack Measurement," these proceedings and references cited therein.
10. S. K. Burke, "A Perturbation Method for Calculating Coil Impedance in Eddy Current Testing," J. Phys. D: Appl. Phys. 18, 1745 (1985).
11. J. D. Jackson, Classical Electrodynamics (Wiley, New York, 1962), pp. 236-239.
12. T. B. A. Senior, Appl. Sci. Res. B 8, 418 (1960).
13. A. Nicholas, "3D Eddy Current Solutions by BIE Techniques," IEEE Trans. Mag. MAG-24, 130 (1988).
14. A. J. Poggio and E. K. Miller, "Integral Equation Solutions of Three-Dimensional Scattering Problems," in Computer Techniques in Electromagnetics, edited by R. Mittra (Pergamon, New York, 1973), p. 159.